Hindawi Publishing Corporation
International Journal of Photoenergy
Volume 2012, Article ID 303961, 9 pages
doi:10.1155/2012/303961

Research Article

A New Photocatalytic System Using Steel Mesh and Cold Cathode Fluorescent Light for the Decolorization of Azo Dye Orange G

Ming-Chin Chang,[1] Chin-Pao Huang,[2] Hung-Yee Shu,[1] and Yung-Chen Chang[1]

[1] *Institute of Environmental Engineering, Hungkuang University, 34 Chung-Chie Road, Shalu, Taichung 433, Taiwan*
[2] *Department of Civil and Environmental Engineering, University of Delaware, Newark, DE 19716, USA*

Correspondence should be addressed to Hung-Yee Shu, hyshu@sunrise.hk.edu.tw

Received 1 June 2012; Accepted 23 June 2012

Academic Editor: Mika Sillanpää

High color and organic composition, the effluents from the textile dyeing and finishing industry, can be treated by photocatalytic oxidation with UV/TiO_2. The objective of this study was to prepare a new photocatalytic system by coating nanosized TiO_2 particles on steel mesh support and using cold cathode fluorescent light (CCFL) irradiation at 365 nm in a closed reactor for the oxidation of azo dye C.I. Orange G (OG). Various factors such as reaction time, coating temperature, TiO_2 dosage, pH, initial dye concentration, and service duration were studied. Results showed efficient color removal of the OG azo dye by the photocatalytic system with TiO_2-coated temperature at 150°C. The optimal TiO_2 dosage for color removal was 60 g m^{-2}. An acidic pH of 2.0 was sufficient for photocatalytic oxidation whereas basic condition was not. The rate of color removal decreased with increase in the initial dye concentration. The TiO_2-coated steel mesh can be used repeatedly over 10 times without losing the photocatalytic efficiency. Results of FTIR and IC indicated the breakage of N=N bonds, with sulfate as the major and nitrite and nitrate as the minor products, which implied degradation of dye molecules.

1. Introduction

Most dyestuffs from the effluent of textile dyeing and finishing industry are organic compounds with high color intensity, recalcitrant to conventional biological wastewater treatment, and thus of major environmental concerns [1–4]. Furthermore, chemical coagulation integrated with activated sludge process was not able to meet the increasingly stringent criteria of color in dye wastewater treatment in Taiwan [5]. There is great demand of technology to decolorize the highly colored dye wastewater more effectively. Azo dyes with nitrogen double bond N=N are the largest class of commercial dyestuffs used in the textile industries. There were reports of successful color removal with final mineralization from azo dye wastewater using advanced oxidation processes (AOPs) such as UV/H_2O_2 [6–9], UV/O_3 [10, 11], or Fenton reaction [12, 13]. Additionally, it has been reported that photocatalytic processes such as UV-TiO_2 system can also be effective in treating dye wastewaters [14–18] except that when applied in suspension further separation of TiO_2 particles is necessary. Therefore, fixing the TiO_2 particles onto supported materials such as silica gel and plates can avoid the particle separation step and enables the easy operation of heterogeneous TiO_2 photocatalysis [19–23]. The objective of this study was to study the degradation of azo dye C.I. Orange G (OG) using a batch photocatalytic reactor in which the photocatalytic TiO_2 particles were coated on steel mesh and cold cathode fluorescent lamp (CCFL) was used (wavelength of 365 nm) as the source of irradiation. The CCFL lamp has thin and simple structure, is less temperature sensitive, and is easy to configure as well as it is brighter than the traditional mercury arc mercury lamp. It is more durable than other light sources. CCFL light is time-saving and less cost which is used broadly in computer products and applications such as liquid crystal display (LCD) backlight displays, PC case lights, and scanners, photocopy machines, industry machines such as appliance lighting, automotive fittings such as dashboard backlights, decoration light, advertisement such as signage board, exit light, and light box, and decoration such as indoors light and

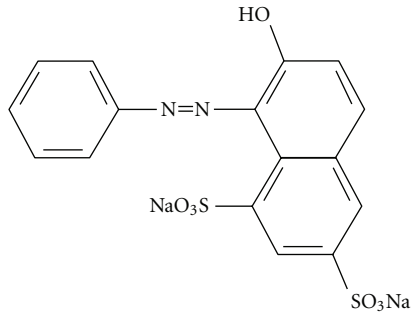

Figure 1: The chemical structure of monoazo dye Orange G. ($C_{16}H_{10}N_2Na_2O_7S_2$).

outdoors light. Factors such as coating temperature, TiO_2 dosage, pH, initial dye concentration, and reaction time that may affect the degree of the dye degradation were studied. Changes in color intensity, pH, and ORP were monitored in addition to the analysis of reaction products by FTIR and IC.

2. Materials and Methods

2.1. Materials and Apparatus. The monoazo dye, C.I. Orange G (OG, $C_{16}H_{10}N_2Na_2O_7S_2$, 60%) with a molecular weight of 452.38 and a characteristic wavelength (λ_{max}) of 479 nm was purchased from Sigma-Aldrich, Inc., and used as received without further purification. Figure 1 shows the chemical structure of OG. The commercial nanosized titanium dioxide (TiO_2), Degussa P-25, with a specific surface area of 48.68 $m^2\,g^{-1}$ from Aldrich was used as the catalyst. The steel mesh (mesh size number 140, 0.106 mm) was purchased from a local hardware store and trimmed into pieces with a gross area of 252 cm^2 (36 × 7 cm). Initially, the steel mesh was trimmed, washed with distilled water, dried at room temperature (25°C), weighed, and then stored in desiccator for further use. A given amount of Degussa P-25 TiO_2 nanoparticle (e.g., 7.5–50.0 g) was mixed with 250 mL of distilled water to make suspension at concentrations of 30–200 $g\,L^{-1}$. The pretreated steel mesh piece was dipped in the TiO_2 suspension then dried under certain temperature for one hour. The steel mesh piece was then washed with distilled water to remove any loose TiO_2 particles from the surface. The dipping, washing, and drying steps were repeated three times to reach a certain weight of TiO_2 on the steel mesh surface. Table 1 shows the amount of TiO_2 coated on the steel mesh surface (gross area of 252 cm^2) in the range of 0.3025–1.6855 g which yielded specific surface TiO_2 concentration in the range of 12–67 $g\,m^{-2}$. Based on images obtained with Field Emission Scanning Electron Microscope (FESEM), model JEOL 6330CF, of the TiO_2-coated steel mesh, it is seen that TiO_2 particles were uniformly coated on the steel mesh surface as shown in Figure 2. The crystallinity of TiO_2 particles was characterized by XRD (Thin-Film X-ray Diffractometer, X-RAY/TF) which yielded an anatase to rutile ratio of 7 : 3 as expected. Table 2 shows the BET surface area and porosity of TiO_2-coated steel mesh as a function of drying temperature using Micromeritics Gemini V. The

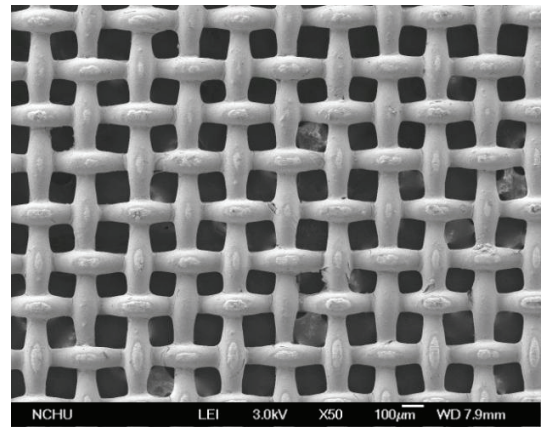

(a)

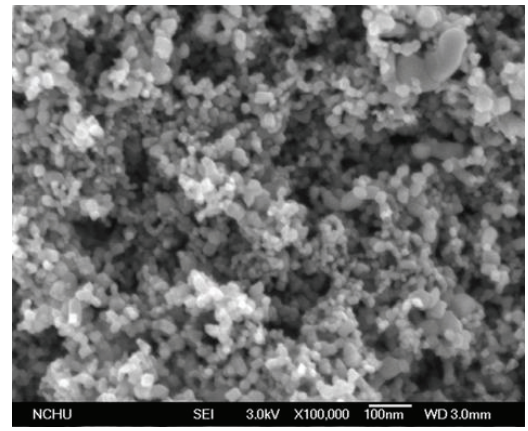

(b)

Figure 2: The morphology of TiO_2 powder coated on steel mesh at 150°C was identified by a JEOL 6330CF Field Emission Scanning Electron Microscope (FESEM). (a) 50 times enlargement and (b) 100,000 times enlargement.

photocatalytic reactor was a closed rectangular black tank (length × width × height equal to 360 × 70 × 78 mm) made of acrylic resin with a removable upper cover underneath of which was six cold cathode fluorescent lamps (CCFL) each of which has a diameter of 0.25 cm, length of 30 cm, light intensity of 4 W, and irradiation wavelength of 365 nm. The dye solution, 200 mL, was introduced to the photocatalytic reactor at which bottom was placed the TiO_2-coated steel mesh with total gross surface area 252 cm^2 (power per unit area of one lamp of 0.35 $mW\,cm^{-2}$); the depth of the dye solution was 0.794 cm neglecting the thickness of the steel mesh. The CCFL lamps were located 6.0 cm above the surface of the dye solution which yielded a total light energy of 2.1 $mW\,cm^{-2}$ measured at the surface of the solution.

2.2. Photocatalytic Procedure. OG azo dye solution at various concentrations was prepared with deionized water. The experimental variables studied included reaction time, TiO_2 dosage, initial dye concentration, and application duration of TiO_2. At a predetermined reaction time, an aliquot of the solution was withdrawn and analyzed for residual

Table 1: The TiO_2-coated weight on the steel meshes.

TiO_2 weight (g) (W_1)	TiO_2 solution concentration (g L^{-1}) (W_1/V)	TiO_2 weight on the coated steel meshes (g) (W_2)	TiO_2 weight per unit area (g m^{-2}) (W_2/A)
7.5	30	0.3025	12
12.5	50	0.5098	20
25.0	100	1.0149	40
37.5	150	1.5054	60
50.0	200	1.6855	67

V: the TiO_2 solution of 250 mL, A: the steel net area of 252 cm^2.

Table 2: The specific surface area and porosity of TiO_2 by various drying temperature for samples with TiO_2 load of 60 g m^{-2}.

Drying temperature °C	Specific surface area m^2 g^{-1}	Porosity Å
100	39.41	9.4077
150	43.35	8.8541
200	49.76	8.4902
250	61.42	9.1983
300	55.35	8.3969

dye concentration, TOC, and color. Dye concentration was determined by measuring the absorbance at wavelength of 479 nm using Hitachi U-2000 spectrophotometer. TOC was obtained with a Total Organic Carbon Analyzer from O.I. Analytical Aurora, model 1030. Color intensity was determined based on the American Dye Manufacturers Institute (ADMI) standard color measurement by applying the Adams-Nickerson color difference formula following method 2120E of the Standard Methods. The pH and redox potential (ORP) were monitored by a Eutech PH5500 dual channel pH/ion meter with specific probes. Besides, the degradation products were identified using Perkin Elmer FT-IR spectrophotometer model Spectrum One. Ions such as sulfate, nitrate, and nitrite were identified with ion chromatography (IC), Dionex ICS-1000.

3. Results and Discussion

3.1. Effect of Combining CCFL UV 365 Irradiation and TiO_2 Catalyst. The color removal was first compared for various systems, that is, CCFL/TiO_2, CCFL alone, and TiO_2 alone at the initial OG concentration of 50 mg L^{-1}, TiO_2 dosage of 60 g m^{-2} and 6 CCFL lamps with total light intensity of 24 W at wavelength of 365 nm in 120 min of reaction in the closed reactor. Figure 3 shows results of color removal by various systems. Results indicated that the system of CCFL alone, and TiO_2 alone could not remove color at any significant level. The CCFL/TiO_2 system removed color and TOC effectively with almost 100 and 95% removal, respectively, in 2 h. It was also observed that the pH remained relatively constant from 5.5 to 5.0 with time. This was expected as TiO_2 is a known photocatalyst that upon radiation with light which wavelength is shorter than that of its bandgap can generate hydroxyl radicals, strong oxidation agents that can oxidize a wide group of organic compounds nonspecifically [14–18].

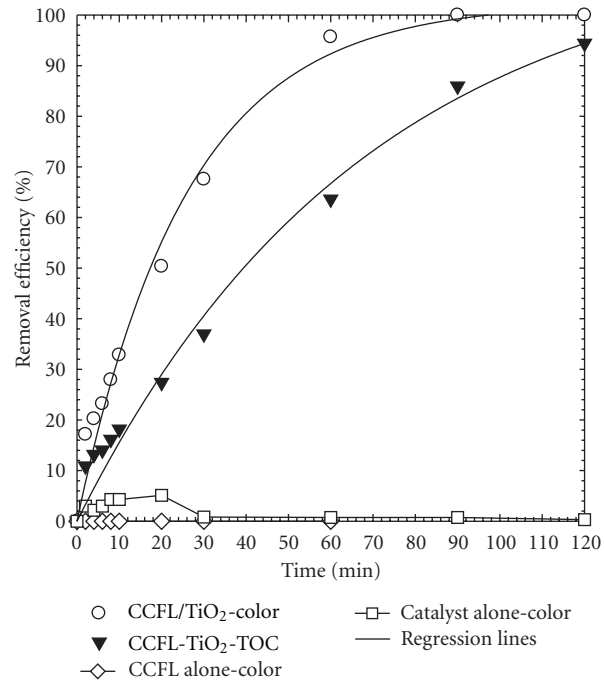

Figure 3: Effect of combining CCFL UV 365 irradiation and TiO_2 catalyst. The conditions were initial dye concentration of 50 mg L^{-1}, TiO_2 coated amounts of 60 g m^{-2}, light intensity of 2.1 mW cm^{-2}, and reaction time during 120 min.

3.2. Effect of Coating Temperature. The effect of TiO_2-coating temperature on color removal was studied at the initial OG concentration of 50 mg L^{-1}, TiO_2 load dosage of 40 g m^{-2} and 6 CCFL lamps in 120 min in the closed reactor. Figure 4 shows insignificant color removal in the range of 100–300°C. It was noted that pH remained unchanged at around 5 to 6. The reaction kinetics of UV/TiO_2 photocatalytical system was proved to follow the Langmuir-Hinshelwood (L-H) reaction kinetics [24–27]. And in most of the designed reaction conditions, the L-H kinetic model of the UV/TiO_2 system can be further simplified into pseudo-first-order reaction kinetics. Therefore, the color removal of this study was treated using pseudo first-order reaction as follows:

$$C_{\text{dye}} = C_{\text{dye0}} \times e^{-kt}, \quad (1)$$

where k denotes the observed first-order reaction rate constant (min^{-1}), t is the reaction time (min), $C_{\text{dye,0}}$ designates

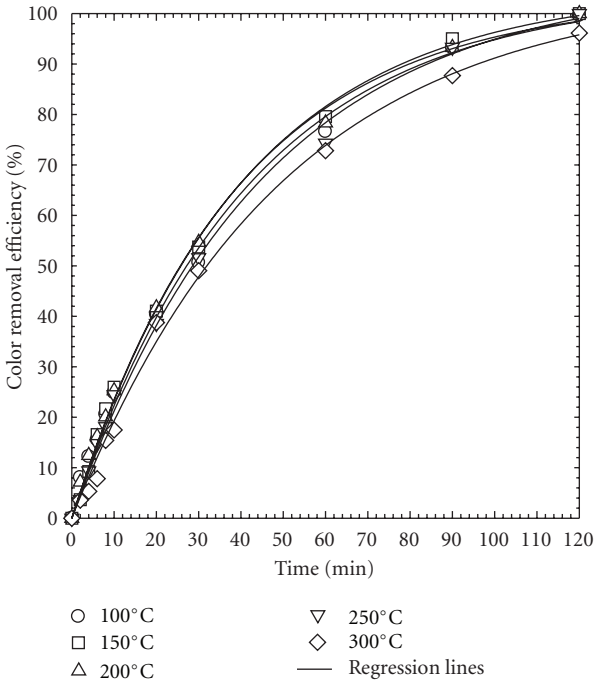

Figure 4: Effect of drying temperature. The conditions were initial dye concentration of 50 mg L^{-1}, TiO_2-coated amounts of 40 g m^{-2}, light intensity of 2.1 mW cm^{-2}, and reaction time during 120 min.

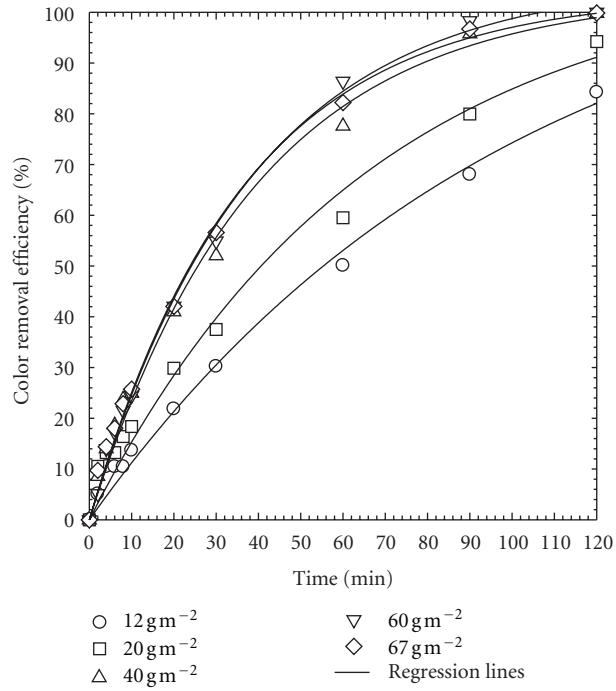

Figure 5: Effect of surface loading of TiO_2. The conditions were initial dye concentration of 50 mg L^{-1}, light intensity of 2.1 mW cm^{-2}, and reaction time during 120 min.

the initial concentration (mg L^{-1}) of OG and $C_{dye,t}$ is the concentration (mg L^{-1}) of OG at time t. The curve fitting of experimental results by (1) were shown in the figures as solid lines to present well-fit of kinetic model to the experimental data. The calculated rate constants (from curve fitting) were 2.36, 2.62, 2.52, 2.27, and 2.23 10^{-2} min^{-1} at 100, 150, 200, 250, and 300°C, respectively, as shown in Table 3(a). The best rate occurred at a coating temperature of 150°C. Note that this temperature was chosen further as the working condition.

3.3. Effect of TiO_2 Load Dosage. Figure 5 shows the removal of color as a function of surface dosage of TiO_2. Results indicated that the color removal increased from 80 to 100% in 120 min when the surface loading of TiO_2 particles increased from 12 to 60 g m^{-2}. The color removal then decreased from 100 to 90% when the surface loading of TiO_2 increased from 60 to 67 g m^{-2}. An optimal TiO_2 loading for color removal occurred at 60 g m^{-2}. The rate constants followed similar trend as percent color removal; the observed rate constants were 1.10, 1.41, 2.41, 3.23, and 2.80 (10^{-2} min^{-1}) at surface TiO_2 loading dosage of 12, 20, 40, 60, and 67 g m^{-2}, respectively, as shown in Table 3(b). Note that the maximum rate constant also occurred at TiO_2 loading of 60 g m^{-2}.

3.4. Effect of pH. The effect of pH on the degradation of azo dye was conducted by adjusting the initial pH value of 5.3 to the range of 2 to 11 using HCl and/or NaOH with initial OG dye concentration of 50 mg L^{-1} and 60 g m^{-2} of TiO_2 dosage. Figure 6 shows the change of dye concentration as a function of time at various pH values. Results indicated that the color removal increased rapidly at acidic pH of 2 and 3 then became slow as the pH increased. This could be attributed to loss of hydroxyl radicals as pH increased. The effect of pH on the photodegradation of acid dye can be better described by the interaction between the dye compound and the photocatalyst. Better contact between the dye chemical and TiO_2 is necessary for the degradation reaction. As pH increases, the surface of TiO_2 becomes negatively charged. (note: the pH_{zpc} of TiO_2 is 5.5). Negatively charged TiO_2 surface discourages the adsorption of the anion acid dye. The rate constants followed similar trend to that of color removal. The rate constants at pH 2 and 3 were 13.28 and 16.6 (10^{-2} min^{-1}), respectively, which were greater than 2.69 (10^{-2} min^{-1}) at pH 4 as shown in Table 3(c). At original pH 5.3, the degradation of OG dye was sufficient fast and reached 100% removal during 120 min reaction time. Furthermore, the effluent from acid dye bath dyeing processing (OG dye was applied) usually presents acidic pH at about 3-4. Thus, it is not suggested that the wastewater treatment plan adjust pH to 2-3 for better treatment efficiency. But it is encouraged to use the advantage of acid dye bath at acidic pH to elevate the reaction rate and removal efficiency.

3.5. Effect of Dye Initial Concentration. To present the validity of L-H model on our CCFL/TiO_2 system, the effect of initial dye concentrations on the photodegradation of azo OG dye was studied at initial concentrations of 12.5–75 mg L^{-1}, TiO_2 dosage of 60 g m^{-2} and 6 CCFL lamps for a period of

Table 3: The first-order reaction rate constant k (10^2 min^{-1}).

(a) Effect of coating temperature		(b) Effect of TiO_2 load dosage		(c) Effect of initial concentration		(d) Effect of initial pH		(e) Duration test	
Temperature, °C	k	Load dosage, g m^{-2}	k	Concentration, mg L^{-1}	k	pH	k	Cycle	k
100	2.36	12	1.10	12.5	12.54	2	13.28	1	3.46
150	2.62	20	1.41	18.8	9.67	3	16.60	2	2.41
200	2.52	40	2.41	25	7.71	4	2.64	3	2.14
250	2.27	60	3.23	50	2.83	5.3	2.69	4	2.06
300	2.23	67	2.80	75	2.0	9	2.67	5	1.62
						11	1.53	6	1.80
								7	1.71
								8	1.73
								9	1.66
								10	1.55

Time for (a) and (b) at 60 min; (c) at 20 min.
Time for (d) at 20 min; (e) at 30 min.

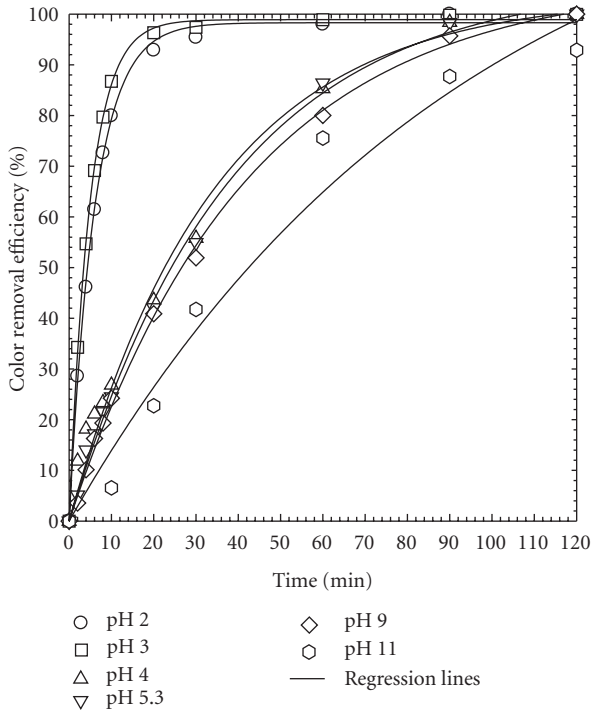

Figure 6: Effect of initial pH. The conditions were TiO_2-coated amounts of 60 g m^{-2}, light intensity of 2.1 mW cm^{-2}, and reaction time during 120 min.

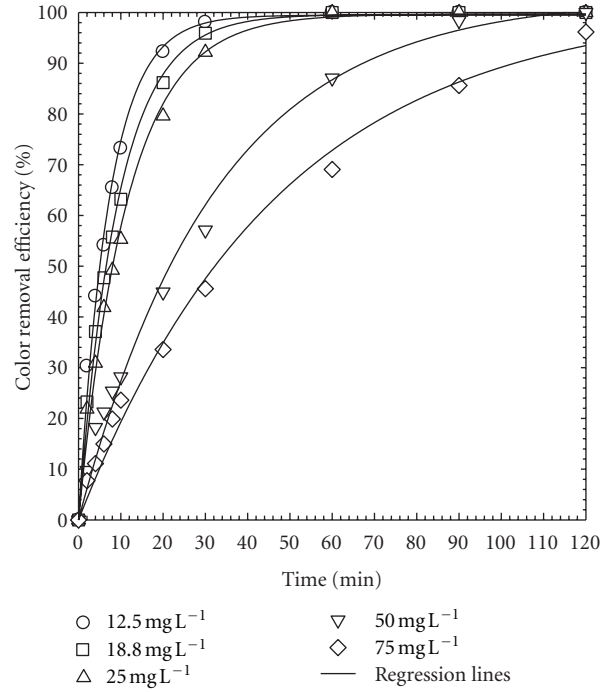

Figure 7: Effect of initial concentration. The conditions were TiO_2-coated amounts of 60 g m^{-2}, light intensity of 2.1 mW cm^{-2}, and reaction time during 0∼120 min.

120 min in the closed reactor. Figure 7 shows results of dye photodegradation as a function of reaction time at various initial dye concentrations. Results indicated that the rate of dye removal decreased from 12.54 to 2.0 (10^{-2} min^{-1}) when the initial dye concentration was increased from 12.5 to 75 mg L^{-1} as shown in Table 3(d). The rate constant then remained constant and independent of the dye concentration as the initial dye concentration increased to greater than 50 mg L^{-1}. This is typical Langmuir-Hinshelwood (L-H) reaction kinetics which is generally capable for modeling UV/TiO_2 photocatalytic oxidation process [24–27]. According to the L-H reaction kinetics, the rate of dye degradation can be described by the following equation:

$$r = \frac{dC}{dt} = \frac{kK_AC}{1 + K_AC}, \tag{2}$$

where r is the degradation rate of dye (mg L^{-1} min^{-1}), k, K_A, and C are the rate constant (mg L^{-1} min^{-1}), equilibrium adsorption constant (L mg^{-1}), and residual dye concentration (mg L^{-1}), respectively. According to the above equation, at high dye concentration, that is, $1 \ll KC$, the rate equation is

$$r = k. \tag{3}$$

Likewise, at low dye concentration, that is, $1 \gg KC$, (2) becomes

$$r = kK_AC. \tag{4}$$

That is, as the initial concentration increases, the reaction no longer follows the first order expression; rather it becomes independent of the dye concentration as shows in (3). By rearranging (2), one has

$$\frac{1}{r_0} = \frac{1}{kK_A} \times \frac{1}{C_0} + \frac{1}{k}, \tag{5}$$

where r_0 and C_0 are the initial rate (mg L^{-1} min^{-1}) and initial dye concentration (mg L^{-1}), respectively. A plot of the reciprocals of initial rate and initial concentration yields the rate constant, k, and the adsorption constant, K (Figure 8). The initial rate r_0 was calculated by the first 2 min of Figure 7 with TiO_2 loading dosage at 12 and 60 g m^{-2}, respectively (Table 4). From the slope ($1/kK_A$) and the intercept ($1/k$) of Figure 8, the calculated k and K_A were 2.08 mg L^{-1} min^{-1} and 0.1257 L mg^{-1} for TiO_2 loading dosage at 12 g m^{-2} and 4.41 mg L^{-1} min^{-1} and 0.0346 L mg^{-1} at 60 g m^{-2}, respectively. The rate constants (k) obtained in this work of 2.08 and 4.41 mg L^{-1} min^{-1} were higher than that of previous works [24–27] such as 1.66, 1.67, 0.95, and 0.17 mg L^{-1} min^{-1} for various dyes direct red 16, remazol black 5, procion red MX-5B, and indigo carmine, respectively. Similarly, the equilibrium adsorption constants (K_A) of 0.1257 and 0.0346 L mg^{-1} from this wok were in the range of previous studies, such as 0.0093, 0.072, 0.071, and 0.78 L mg^{-1} for various dyes as above. The results indicate that the photocatalytic degradation of Orange G by CCFL/TiO_2 process followed the Langmuir-Hinshelwood kinetic model.

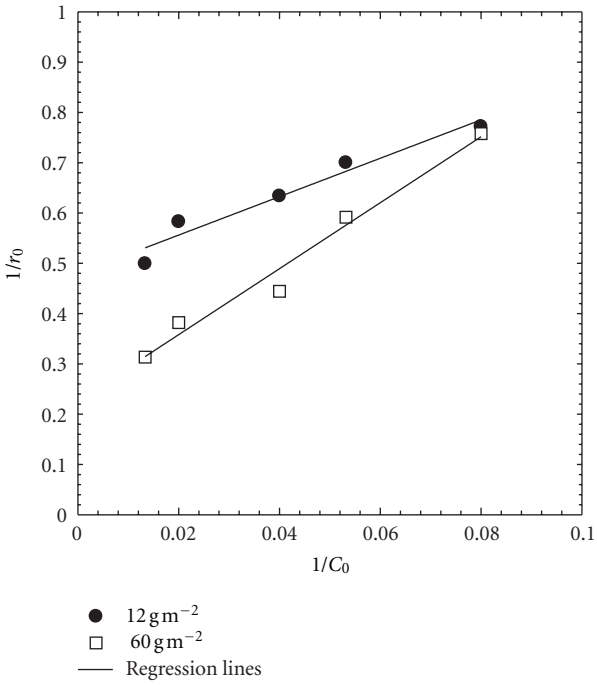

Figure 8: Langmuir-Hinshelwood kinetic model (comparison of two different TiO_2 loading dosage of 12 and 60 g m^{-2} with light intensity of 2.1 mW cm^{-2}).

Table 4: The effect of dye concentration on initial rate r_0 (mg L^{-1} min^{-1}) with TiO_2 loading dosage at 12 and 60 g m^{-2}.

OG concentration, C_0 (mg L^{-1})	12.5	18.8	25	50	75
r_0-12 g m^{-2}	1.30	1.43	1.58	1.72	2.00
r_0-60 g m^{-2}	1.32	1.69	2.25	2.62	3.19

3.6. The Product Analysis by FTIR and IC. The change of functional groups of azo dye after photocatalytic treatment was surveyed. The initial dye concentration was 50 mg L^{-1} and was treated with a TiO_2 dosage of 60 g m^{-2} and reaction time of 120 min. The scan spectra for the functional groups is SO_3Na of 1150~1250 cm^{-1}, N=N of 1400~1500 cm^{-1}, C=O of 1690~1760 cm^{-1}, C–H, and N–H of 3300~3500 cm^{-1}. The residual color was 0 and the residual TOC was 2.13 mg L^{-1}. After the photocatalytic oxidation, a new double-bond C=O at 1637 cm^{-1} was produced. Meanwhile the N=N from dye at 1426, 1463, and 1496 cm^{-1} disappeared due to attack by the hydroxyl radicals that cleaved the double-bond N=N. Accordingly, the dye molecule was degraded and decolorized. The ions such as sulfate, chloride, nitrite, and nitrate were determined. Figure 9 shows that the major ion concentration of sulfate significantly increased to 11 mg L^{-1} over time. The nitrate ion concentration was about 0.4 to 0.5 mg L^{-1} and nitrite concentration was low at 0.1 mg L^{-1}. The chloride ion produced due to the impurity of OG dye was low as 1.5 mg L^{-1}.

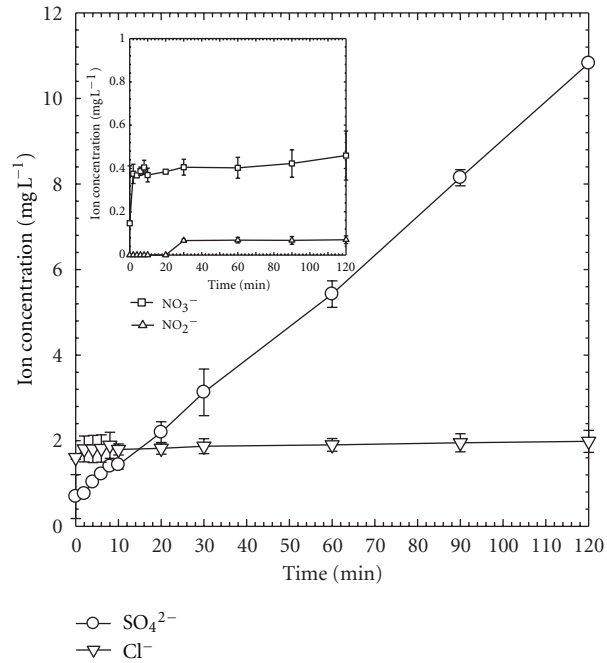

Figure 9: The product analysis by IC. The conditions were initial dye concentration of 50 mg L^{-1}, TiO_2-coated amounts of 60 g m^{-2}, and light intensity of 2.1 mW cm^{-2} at 120 min.

3.7. Application Duration. The TiO_2-coated steel mesh was used repeatedly to treat the OG solution. Figure 10 shows the system performance over 10 cycles. Results indicated that although the rate of OG degradation decreased as the reuse cycle of catalyst increased, the total amount of dye removal remained relatively unchanged at 100% in the treatment time range of 100–120 min, however. In the meantime, there was nearly no loss of TiO_2 in each operation even after 10 cycles. The observed rate constants declined with more reuse cycles as shown in Table 3(e), however. This can be attributed to potential surface poisoning of the photocatalyst, TiO_2 due to adsorption of reaction products. Further investigation is in progress to assess the reactivity of the TiO_2 during the course of photocatalytic reactions.

4. Conclusions

TiO_2 supported on steel mesh and illuminated with cold cathode fluorescent light (CCFL) was effective in removal color and dye from the OG azo dye solution. Coating TiO_2 at 150°C yielded the fastest color removal rate. An optimal TiO_2 surface loading or dosage of 60 g m^{-2} exhibited the highest color removal as well as the fastest rate; increase in surface TiO_2 loading had no benefit in increasing the color removal, however. An acidic pH of 2-3 had the best photocatalytic oxidation rate; the rate of color removal decreased when pH was increased to greater than 4. The rate of color removal decreased with initial dye concentration as was expected by the Langmuir-Hinshelwood kinetics. Based on FTIR analysis, there was decrease of N=N bonding which indicated chemical transformation of the dye OG

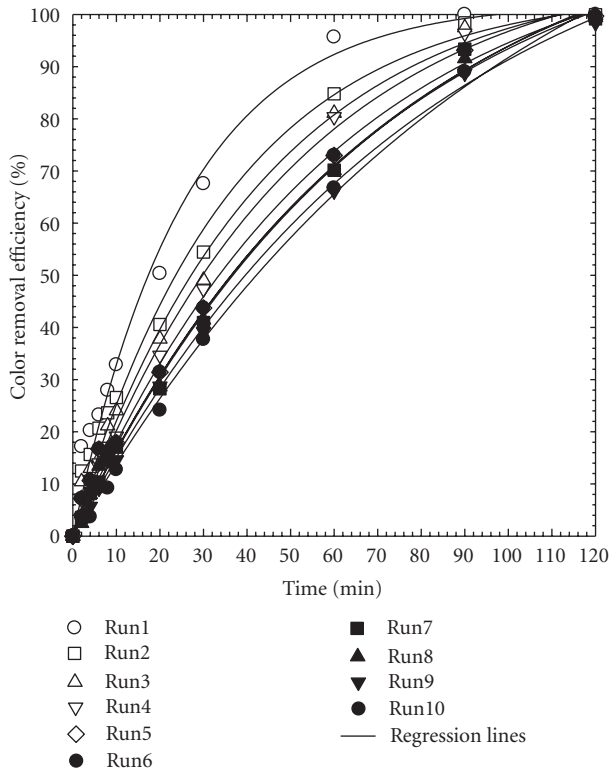

Figure 10: Duration test on color removal. The conditions were initial dye concentration of 50 mg L^{-1}, TiO_2-coated amounts of 60 g m^{-2}, light intensity of 2.1 mW cm^{-2}, and reaction time during 120 min.

compound. Results of analyzing the inorganic byproducts revealed that sulfate production was predominant; nitrite and nitrate were produced at minor quantities. The TiO_2-coated steel mesh can be repeatedly used over 10 cycles without significant loss of catalyst mass; the percent dye removal remained close to 100% in 10 cycles except slight decrease in reaction rate constants apparently due to possible surface poisoning. In general, the new photocatalytic system showed great potential in ease of implementation and cost for the treatment of dye industrial wastewater for color removal.

Acknowledgments

The authors appreciate the partial research funding granted by the Taiwan National Science Foundation (NSC 97-2918-I-241-001 and NSC 96-2221-E-241-005-MY2) as well as the analysis by NSC instrumental center of National Chung Hsing University and National Tsing Hua University.

References

[1] M. A. Brown and S. C. DeVito, "Predicting azo dye toxicity," *Critical Reviews in Environmental Science and Technology*, vol. 23, no. 3, pp. 249–324, 1993.

[2] H. Y. Shu, C. R. Huang, and M. C. Chang, "Decolorization of mono-azo dyes in wastewater by advanced oxidation process: a case study of acid red 1 and acid yellow 23," *Chemosphere*, vol. 29, no. 12, pp. 2597–2607, 1994.

[3] B. Manu and S. Chaudhari, "Decolorization of indigo and azo dyes in semicontinuous reactors with long hydraulic retention time," *Process Biochemistry*, vol. 38, no. 8, pp. 1213–1221, 2003.

[4] J. Ge and J. Qu, "Ultrasonic irradiation enhanced degradation of azo dye on MnO_2," *Applied Catalysis B*, vol. 47, no. 2, pp. 133–140, 2009.

[5] C. M. Kao, M. S. Chou, W. L. Fang, B. W. Liu, and B. R. Huang, "Regulating colored textile wastewater by 3/31 wavelength admi methods in Taiwan," *Chemosphere*, vol. 44, no. 5, pp. 1055–1063, 2001.

[6] H. Y. Shu, M. C. Chang, and H. J. Fan, "Decolorization of azo dye acid black 1 by the UV/H_2O_2 process and optimization of operating parameters," *Journal of Hazardous Materials*, vol. 113, no. 1-3, pp. 201–208, 2004.

[7] H. Y. Shu, M. C. Chang, and H. J. Fan, "Effects of gap size and UV dosage on decolorization of C.I. Acid Blue 113 wastewater in the UV/H_2O_2 process," *Journal of Hazardous Materials*, vol. 118, no. 1–3, pp. 205–211, 2005.

[8] H. Y. Shu, M. C. Chang, and W. P. Hsieh, "Remedy of dye manufacturing process effluent by UV/H_2O_2 process," *Journal of Hazardous Materials*, vol. 128, no. 1, pp. 60–66, 2006.

[9] E. Rodríguez, R. Peche, J. M. Merino, and L. M. Camarero, "Decoloring of aqueous solutions of indigocarmine dye in an acid medium by H_2O_2/UV advanced oxidation," *Environmental Engineering Science*, vol. 24, no. 3, pp. 363–371, 2007.

[10] H. Y. Shu and M. C. Chang, "Decolorization effects of six azo dyes by O_3, UV/O_3 and UV/H_2O_2 processes," *Dyes and Pigments*, vol. 65, no. 1, pp. 25–31, 2005.

[11] C. H. Wu and H. Y. Ng, "Degradation of C.I. Reactive Red 2 (RR2) using ozone-based systems: comparisons of decolorization efficiency and power consumption," *Journal of Hazardous Materials*, vol. 152, no. 1, pp. 120–127, 2008.

[12] T. H. Kim, C. Park, J. Yang, and S. Kim, "Comparison of disperse and reactive dye removals by chemical coagulation and Fenton oxidation," *Journal of Hazardous Materials*, vol. 112, no. 1-2, pp. 95–103, 2004.

[13] F. Ay, E. C. Catalkaya, and F. Kargi, "Advanced oxidation of direct red (DR 28) by fenton treatment," *Environmental Engineering Science*, vol. 25, no. 10, pp. 1455–1462, 2008.

[14] A. T. Toor, A. Verma, C. K. Jotshi, P. K. Bajpai, and V. Singh, "Photocatalytic degradation of Direct Yellow 12 dye using UV/TiO_2 in a shallow pond slurry reactor," *Dyes and Pigments*, vol. 68, no. 1, pp. 53–60, 2006.

[15] M. Muruganandham and M. Swaminathan, "Photocatalytic decolourisation and degradation of Reactive Orange 4 by TiO_2-UV process," *Dyes and Pigments*, vol. 68, no. 2-3, pp. 133–142, 2006.

[16] X. Yin, F. Xin, F. Zhang, S. Wang, and G. Zhang, "Kinetic study on photocatalytic degradation of 4BS Azo dye over TiO_2 in slurry," *Environmental Engineering Science*, vol. 23, no. 6, pp. 1000–1008, 2006.

[17] A. Akyol and M. Bayramoglu, "The degradation of an azo dye in a batch slurry photocatalytic reactor," *Chemical Engineering and Processing*, vol. 47, no. 12, pp. 2150–2156, 2008.

[18] R. B. M. Bergamini, E. B. Azevedo, and L. R. R. D. Araújo, "Heterogeneous photocatalytic degradation of reactive dyes in aqueous TiO_2 suspensions: decolorization kinetics," *Chemical Engineering Journal*, vol. 149, no. 1–3, pp. 215–220, 2009.

[19] G. Mascolo, R. Comparelli, M. L. Curri, G. Lovecchio, A. Lopez, and A. Agostiano, "Photocatalytic degradation of methyl red by TiO_2: comparison of the efficiency of immobilized nanoparticles versus conventional suspended catalyst,"

Journal of Hazardous Materials, vol. 142, no. 1-2, pp. 130–137, 2007.

[20] B. Mounir, M. N. Pons, O. Zahraa, A. Yaacoubi, and A. Benhammou, "Discoloration of a red cationic dye by supported TiO_2 photocatalysis," *Journal of Hazardous Materials*, vol. 148, no. 3, pp. 513–520, 2007.

[21] M. Nikazar, K. Gholivand, and K. Mahanpoor, "Photocatalytic degradation of azo dye Acid Red 114 in water with TiO_2 supported on clinoptilolite as a catalyst," *Desalination*, vol. 219, no. 1–3, pp. 293–300, 2008.

[22] A. R. Khataee, M. N. Pons, and O. Zahraa, "Photocatalytic degradation of three azo dyes using immobilized TiO_2 nanoparticles on glass plates activated by UV light irradiation: influence of dye molecular structure," *Journal of Hazardous Materials*, vol. 168, no. 1, pp. 451–457, 2009.

[23] X. Wang, Y. Liu, Z. Hu, Y. Chen, W. Liu, and G. Zhao, "Degradation of methyl orange by composite photocatalysts nano-TiO_2 immobilized on activated carbons of different porosities," *Journal of Hazardous Materials*, vol. 169, no. 1–3, pp. 1061–1067, 2009.

[24] T. Aarthi, P. Narahari, and G. Madras, "Photocatalytic degradation of Azure and Sudan dyes using nano TiO_2," *Journal of Hazardous Materials*, vol. 149, no. 3, pp. 725–734, 2007.

[25] K. Sahel, N. Perol, H. Chermette, C. Bordes, Z. Derriche, and C. Guillard, "Photocatalytic decolorization of Remazol Black 5 (RB5) and Procion Red MX-5B-Isotherm of adsorption, kinetic of decolorization and mineralization," *Applied Catalysis B*, vol. 77, no. 1-2, pp. 100–109, 2007.

[26] N. Barka, A. Assabbane, A. Nounah, and Y. A. Ichou, "Photocatalytic degradation of indigo carmine in aqueous solution by TiO_2-coated non-woven fibres," *Journal of Hazardous Materials*, vol. 152, no. 3, pp. 1054–1059, 2008.

[27] J. Saien, M. Asgari, A. R. Soleymani, and N. Taghavinia, "Photocatalytic decomposition of direct red 16 and kinetics analysis in a conic body packed bed reactor with nanostructure titania coated Raschig rings," *Chemical Engineering Journal*, vol. 151, no. 1–3, pp. 295–301, 2009.